

Thermodynamics of Reissner-Nordström-anti-de Sitter black holes in the grand canonical ensemble

Claudia S. Peça

Departamento de Física, Instituto Superior Técnico, Av. Rovisco Pais 1, 1096 Lisboa Codex, Portugal

José P. S. Lemos

*Departamento de Astrofísica, Observatório Nacional-CNPq, Rua General José Cristino 77, 20921 Rio de Janeiro, Brazil
and Departamento de Física, Instituto Superior Técnico, Av. Rovisco Pais 1, 1096 Lisboa Codex, Portugal*

(February 5, 2020)

The thermodynamical properties of the Reissner-Nordström-anti-de Sitter black hole in the grand canonical ensemble are investigated using York's formalism. The black hole is enclosed in a cavity with finite radius where the temperature and electrostatic potential are fixed. The boundary conditions allow us to compute the relevant thermodynamical quantities, e.g. thermal energy, entropy and charge. The stability conditions imply that there are thermodynamically stable black hole solutions, under certain conditions. Instantons with negative heat capacity are also found.

I. INTRODUCTION

The path-integral approach to the thermodynamics of black holes was originally developed by Hawking *et al.* [1–3]. In this approach the thermodynamical partition function is computed from the path-integral in the saddle-point approximation, thus obtaining the thermodynamical laws for black holes.

In the path-integral approach we can use the three different ensembles: microcanonical, canonical and grand canonical. Due to difficulties related to stability of the black hole in the canonical ensemble, the microcanonical ensemble was originally considered [3,4]. However, further developments by York *et al.* [5–8] allowed to define the canonical ensemble correctly. Effectively, by carefully defining the boundary conditions, one can properly obtain the partition function of a black hole in thermodynamical equilibrium. This approach was further developed to include other ensembles [9], and to study charged black holes in the grand canonical ensemble [10] and black holes in asymptotically anti-de Sitter spacetimes [11,12]. This approach was also applied to black holes in two [13] and three [11] dimensions.

In York's formalism the black hole is enclosed in a cavity with a finite radius. The boundary conditions are defined according to the thermodynamical ensemble under study. Given the boundary conditions and imposing the appropriate constraints, one can compute a reduced action suitable for doing black hole thermodynamics [10,14]. Evaluating this reduced action at its stable stationary point one obtains the corresponding classical action, which is related to a thermodynamical potential. In the canonical ensemble this thermodynamical potential corresponds to the Helmholtz free energy, while for the grand canonical ensemble the thermodynamical potential is the grand canonical potential [2,10]. From the thermodynamical potential one can compute all the relevant thermodynamical quantities and relations [15].

Some controversy has appeared related to the boundary conditions chosen in this formalism [11,16,17]. More precisely, Hawking and Page [16,17] fix the Hawking temperature of the black hole (i.e. the temperature defined so that the respective Euclidean metric has no conical singularity at the horizon) at infinity, while York *et al.* [5,10,11] fix the local temperature at a finite radius, where the boundary conditions are defined. For asymptotically flat spacetimes the two formalism coincide, because at infinity the local temperature is equal to the Hawking temperature. On the contrary, for asymptotically anti-de Sitter spacetimes the two procedures disagree, since the local temperature is redshifted to zero at infinity and is equal to the Hawking temperature only in the region where spacetime has a flat metric. Louko and Winters-Hilt [12] have studied the thermodynamics of the Reissner-Nordström-anti-de Sitter black hole fixing a renormalized temperature at infinity that corresponds to the same procedure used in [16,17]. In this paper we have chosen to follow York's formalism [5,10,11] and study the thermodynamics of the Reissner-Nordström-anti-de Sitter black hole fixing the local temperature at finite radius.

We find that the two procedures give some identical results, e.g., in both procedures the Hawking-Bekenstein formula for the entropy [18,19] is obtained. However, the value for the energy at infinity differs depending on which procedures one uses. In [12] it was found that the energy at infinity is equal to the mass of the black hole, a result that does not

hold here. These results conform with the similarities and differences found for the Schwarzschild-anti-de Sitter black hole in [16,11].

II. THE ACTION

The Euclidean action in general relativity [3] is given by

$$I = -\frac{1}{16\pi} \int_{\mathcal{M}} d^4x \sqrt{g} (R - 2\Lambda) + \frac{1}{8\pi} \int_{\partial\mathcal{M}} d^3x \sqrt{h} K - \int_{\mathcal{M}} d^4x \sqrt{g} L_m - I_{\text{subtr}} , \quad (1)$$

where \mathcal{M} is a compact region with boundary $\partial\mathcal{M}$, R is the scalar curvature, Λ the cosmological constant, g the determinant of the Euclidean metrics, K the trace of the extrinsic curvature of the boundary $\partial\mathcal{M}$, h is the determinant of the Euclidean induced metrics on the boundary, L_m the Euclidean Lagrangian density of the matter fields and I_{subtr} is an arbitrary term that can be used to define the zero of the energy as will be seen later.

In order to set the nomenclature we follow [10] in this section. We consider a spherical symmetric static metric of the form [10]

$$ds^2 = b^2 d\tau^2 + a^2 dy^2 + r^2 d\Omega^2 , \quad (2)$$

where a , b and r are functions only of the radial coordinate $y \in [0, 1]$. The Euclidean time τ has period 2π . The event horizon, given by $y = 0$, has radius $r_+ = r(0)$ and area $A_+ = 4\pi r_+^2$. The boundary is given by $y = 1$ and at this boundary the thermodynamical variables defining the ensemble are fixed. The boundary is a two-sphere with area $A_B = 4\pi r_B^2$, where $r_B = r(1)$. We will consider the grand canonical ensemble, where heat and charge can flow in and out through the boundary to maintain a constant temperature $T \equiv T(r_B)$ and electrostatic potential $\phi \equiv \phi(r_B)$ at the boundary.

Imposing a black hole topology to the metric (2), one obtains the regularity conditions, see [10],

$$b(0) = 0 \quad (3)$$

and

$$\left. \frac{b'}{a} \right|_{y=0} = 1 . \quad (4)$$

Furthermore, the Euler number for this topology must be $\chi = 2$. Using the Gauss-Bonnet-Chern formula [20], one has

$$\chi = 2 \left\{ \frac{b'}{a} \left[1 - \left(\frac{r'}{a} \right)^2 \right] \right\} \Big|_{y=0} = 2 \quad \Rightarrow \quad \left. \frac{r'^2}{a^2} \right|_{y=0} = 0 . \quad (5)$$

This corresponds to the usual coordinate singularity that occurs at the black hole horizon $g_{rr}^{-1}|_{r=r_+}$.

The inverse temperature at the boundary is given by the proper length of the time coordinate at the boundary,

$$\beta \equiv T^{-1} = \int_0^{2\pi} b(1) d\tau = 2\pi b(1) . \quad (6)$$

Evaluating the gravitational part I_g of the action (1) for the metric (2), using conditions (3-6) yields

$$\begin{aligned} I_g &= -\frac{1}{16\pi} \int_{\mathcal{M}} d^4x \sqrt{g} (R - 2\Lambda) + \frac{1}{8\pi} \int_{\partial\mathcal{M}} d^3x \sqrt{h} K - I_{\text{subtr}} \\ &= \frac{1}{2} \int_0^{2\pi} d\tau \int_0^1 dy \left(-2 \frac{r b' r'}{a} - \frac{b r'^2}{a} - a b + \Lambda a b r^2 \right) - \frac{1}{2} \int_0^{2\pi} d\tau \left. \frac{(b r^2)'}{a} \right|_{y=0} - I_{\text{subtr}} . \end{aligned} \quad (7)$$

The matter field considered in this paper is the electromagnetic field only, therefore the matter field action $I_m = -\int_{\mathcal{M}} d^4x \sqrt{g} L_m$ used will be the Euclidean Maxwell action

$$I_m = \frac{1}{16\pi} \int_{\mathcal{M}} d^4x \sqrt{g} F_{\mu\nu} F^{\mu\nu} . \quad (8)$$

where $F_{\mu\nu}$ is the Faraday tensor

$$F_{\mu\nu} = \partial_\mu A_\nu - \partial_\nu A_\mu \quad (9)$$

and A_μ the electromagnetic 4-potential. The action term I_m given in (8) corresponds to the action term for the grand canonical ensemble with the electromagnetic potential A_μ fixed at the boundary.

Due to the spherical and static symmetry, the electromagnetic potential can be written as

$$A_\mu dx^\mu = A_\tau(y) d\tau . \quad (10)$$

Therefore I_m given in (8) is equal to,

$$I_m = \frac{1}{2} \int_0^{2\pi} d\tau \int_0^1 dy \frac{r^2}{ab} A'_\tau{}^2 . \quad (11)$$

In order to obtain the reduced action one uses the proper constraints. For the gravitational part of the action I_g given in (7), the constraint used is the Hamiltonian constraint [10,14]

$$G^\tau{}_\tau + \Lambda g^\tau{}_\tau = 8\pi T^\tau{}_\tau . \quad (12)$$

In addition, for the matter fields part of the action I_m given in (11) we use the Gauss's-law constraint, which is, in the case of a spherical and static symmetry, the only nontrivial Maxwell equation and therefore it is given by

$$F^{\mu\nu}{}_{;\nu} = 0 \quad \Rightarrow \quad \frac{r^2}{ab} A'_\tau = \text{cte} . \quad (13)$$

The thermodynamical quantities and relations are obtained from the ‘‘classical action’’ \tilde{I} (defined as the reduced action evaluated at its locally stable stationary points) using the well known relation between the ‘‘classical action’’ and the thermodynamical potential

$$\tilde{I} = \beta F . \quad (14)$$

Here F is the grand canonical potential since we are considering the grand canonical ensemble. All the thermodynamical quantities can be obtained from F using the classical thermodynamical relations (see for example [15]).

III. THE REISSNER-NORDSTRÖM-ANTI-DE SITTER BLACK HOLE

The Reissner-Nordström-anti-de Sitter black hole in the grand canonical ensemble is obtained using a negative cosmological constant Λ and the boundary conditions $T \equiv T(R_B)$ and $\phi \equiv \phi(r_B)$, where r_B is the boundary radius of the spherical cavity, T the temperature at the boundary and ϕ the electrostatic potential difference between the horizon and the boundary. Instead of T we can also use its inverse β .

The reduced action for Reissner-Nordström-anti-de Sitter black hole is obtained from the Euclidean Einstein-Hilbert-Maxwell action I given in (1), where the term that corresponds to the matter fields is the Euclidean Maxwell action given in (8). As in section II, we split the action in two terms $I = I_g + I_m$, where I_g is the gravitational term given in (7) and I_m the matter field term given in (11). To obtain the reduced action we use the Hamiltonian constraint (12) and the Gauss's constraint (13).

The evaluation of I_A is identical to the case $\Lambda = 0$ and can therefore be found in [10],

$$I_A = -\frac{1}{2} \beta e \phi , \quad (15)$$

where e is the electrical charge of the black hole and ϕ is the difference of potential between $y = 0$ and $y = 1$ ($A_\tau(1) = \frac{\beta\phi}{2\pi i}$). To evaluate the gravitational term I_g (7) we use as mentioned above the constraint (12)

$$G^\tau{}_\tau + \Lambda g^\tau{}_\tau = 8\pi T^\tau{}_\tau . \quad (16)$$

The stress-energy tensor component $T^\tau{}_\tau$ is given by

$$T^\tau{}_\tau = -\frac{1}{8\pi} \frac{e^2}{r^4} . \quad (17)$$

The component of the Einstein tensor $G^\tau{}_\tau$ for the metric (2) is

$$G^\tau{}_\tau = \frac{r'^2}{a^2 r^2} - \frac{1}{r^2} + \frac{2r''}{a^2 r} - \frac{2a'r'}{a^3 r}. \quad (18)$$

Substituting (17) and (18) in (16) we obtain

$$\Lambda = -\frac{e^2}{r^4} - \frac{r'^2}{a^2 r^2} + \frac{1}{r^2} - \frac{2r''}{a^2 r} + \frac{2a'r'}{a^3 r}. \quad (19)$$

Rearranging terms in equation (19)

$$\frac{1}{r^2 r'} \left\{ \left[r \left(\frac{r'^2}{a^2} - 1 \right) \right]' + \frac{e^2 r'}{r^2} + \Lambda r^2 r' \right\} = 0. \quad (20)$$

Integrating and simplifying the previous equation yields

$$\left(\frac{r'}{a} \right)^2 = 1 - \frac{2M}{r} + \frac{e^2}{r^2} + \alpha^2 r^2, \quad (21)$$

where $2M$ is an integration constant and $\alpha^2 = -\Lambda/3$. The integration constant $2M$ can be evaluated using the condition that the Euler number be $\chi = 2$. Equation (5) reveals

$$2M = r_+ + \frac{e^2}{r_+} + \alpha^2 r_+^3. \quad (22)$$

This is the known relation between the ADM mass of the Reissner-Nordström-anti-de Sitter black hole and its event horizon radius.

Substituting (19) in (7) yields

$$\begin{aligned} I_g^* &= \frac{1}{2} \int_0^{2\pi} d\tau \int_0^1 dy \left(-2 \frac{r b' r'}{a} - 2 \frac{b r'^2}{a} - 2 \frac{b r r''}{a} + 2 \frac{b r a' r'}{a^2} - e^2 \frac{a b}{r^2} \right) - \\ &\quad - \frac{1}{2} \int_0^{2\pi} d\tau \left. \frac{(b r^2)'}{a} \right|_{y=0} - I_{\text{subtr}} \\ &= - \int_0^{2\pi} d\tau \int_0^1 dy \left(\frac{b r r'}{a} \right)' - \frac{1}{2} \int_0^{2\pi} d\tau \int_0^1 dy e^2 \frac{a b}{r^2} - \\ &\quad - \frac{1}{2} \int_0^{2\pi} d\tau \left. \frac{b' r^2}{a} \right|_{y=0} - I_{\text{subtr}}, \end{aligned} \quad (23)$$

where we have used (3).

The first term after the second equality in equation (23) can be evaluated by integrating and substituting equations (21) and (22). To evaluate the respective second term, we compare it to (11) and use $\frac{r^2}{ab} A'_\tau = -i e$ [10], and conclude that it is equal to I_A given in (15). The respective third term is integrated and gives $-\pi r_+^2$. Following this procedure, we obtain

$$I_g^* = -\beta r_B \sqrt{1 - \frac{r_+}{r_B} - \frac{e^2}{r_+ r_B} - \alpha^2 \frac{r_+^3}{r_B} + \frac{e^2}{r_B^2} + \alpha^2 r_B^2} - \frac{1}{2} \beta e \phi - \pi r_+^2 - I_{\text{subtr}}, \quad (24)$$

where conditions (3), (4) and (6) were used.

Adding (15) and (24), yields the reduced action

$$I^* = -\beta r_B \sqrt{1 - \frac{r_+}{r_B} - \frac{e^2}{r_+ r_B} - \frac{\alpha^2 r_+^3}{r_B} + \frac{e^2}{r_B^2} + \alpha^2 r_B^2} - \beta e \phi - \pi r_+^2 - I_{\text{subtr}}. \quad (25)$$

The term I_{subtr} is of the form βE_{subtr} , where E_{subtr} is a constant that does not depend on β or ϕ , since I_{subtr} is an arbitrary term that can be used to fix the zero of the energy but cannot affect other thermodynamical variables [5]. For convenience, we use for the zero of the energy

$$E_{\text{ADS}} = E(r_+ = 0, e = 0) = 0, \quad (26)$$

where E_{ADS} is the thermal energy of anti-de Sitter spacetime.

To evaluate I_{subtr} , we compute the thermal energy of the Reissner-Nordström-anti-de Sitter black hole from (25) and use condition (26). The thermal energy is given by [15]

$$\begin{aligned} E &= F + \beta \left(\frac{\partial F}{\partial \beta} \right)_{\phi, r_B} - \left(\frac{\partial F}{\partial \phi} \right)_{\beta, r_B} \phi = \left(\frac{\partial \tilde{I}}{\partial \beta} \right)_{\phi, r_B} - \frac{\phi}{\beta} \left(\frac{\partial \tilde{I}}{\partial \phi} \right)_{\beta, r_B} = \\ &= -r_B \sqrt{1 - \frac{r_+}{r_B} - \frac{e^2}{r_+ r_B} - \frac{\alpha^2 r_+^3}{r_B} + \frac{e^2}{r_B^2} + \alpha^2 r_B^2} - E_{\text{subtr}} \end{aligned} \quad (27)$$

where F is the grand canonical potential and we have used (14). Although the reduced action I^* is not the classical action (therefore we cannot write $I^* = \beta F$), the energy has the form given in (27). This is because the classical action \tilde{I} corresponds to the minimum of the reduced action and therefore the equalities $\left(\frac{\partial \tilde{I}}{\partial \beta} \right)_{\phi, r_B} = \left(\frac{\partial I^*}{\partial \beta} \right)_{\phi, r_B, r_+, e}$ and $\left(\frac{\partial \tilde{I}}{\partial \phi} \right)_{\beta, r_B} = \left(\frac{\partial I^*}{\partial \phi} \right)_{\beta, r_B, r_+, e}$ hold. However, r_+ and e in (27) are not free parameters, they depend on the boundary conditions (i.e. on the values of β , ϕ and r_B) and on the cosmological constant. The functions $r_+ = r_+(\beta, \phi, r_B, \alpha)$ and $e = e(\beta, \phi, r_B, \alpha)$ are obtained from the equilibrium conditions $\frac{\partial I^*}{\partial r_+} = 0$ and $\frac{\partial I^*}{\partial e} = 0$ as will be seen later.

Using equation (26) on (27), yields

$$E_{\text{subtr}} = -r_B \sqrt{1 + \alpha^2 r_B^2}. \quad (28)$$

Substituting (28) in (25), we finally obtain the reduced action for the Reissner-Nordström-anti-de Sitter black hole

$$I^* = \beta r_B \left(\sqrt{1 + \alpha^2 r_B^2} - \sqrt{1 - \frac{r_+}{r_B} - \frac{e^2}{r_+ r_B} - \frac{\alpha^2 r_+^3}{r_B} + \frac{e^2}{r_B^2} + \alpha^2 r_B^2} \right) - \beta e \phi - \pi r_+^2. \quad (29)$$

Similarly substituting (28) in (27), we obtain its thermal energy

$$E = r_B \left(\sqrt{1 + \alpha^2 r_B^2} - \sqrt{1 - \frac{r_+}{r_B} - \frac{e^2}{r_+ r_B} - \frac{\alpha^2 r_+^3}{r_B} + \frac{e^2}{r_B^2} + \alpha^2 r_B^2} \right). \quad (30)$$

The mean value of the charge is

$$Q = - \left(\frac{\partial F}{\partial \phi} \right)_{\beta, r_B} = -\frac{1}{\beta} \left(\frac{\partial \tilde{I}}{\partial \phi} \right)_{\beta, r_B} = e. \quad (31)$$

The entropy is obtained from

$$S = \beta^2 \left(\frac{\partial F}{\partial \beta} \right)_{\phi, r_B} = \beta \left(\frac{\partial \tilde{I}}{\partial \beta} \right)_{\phi, r_B} - \tilde{I} = \pi r_+^2, \quad (32)$$

where equation (14) was used. Since $A_+/4 = \pi r_+^2$, where A_+ is the area of the event horizon, this is the usual Hawking-Bekenstein entropy [18,19].

As mentioned above, the event horizon radius r_+ and electric charge e of the black hole for the given boundary conditions, i.e. β , ϕ and r_B , are obtained by evaluating the locally stable stationary points of the reduced action with respect to r_+ and e [10]. Effectively, once the values of β , ϕ and r_B are held fixed by the boundary conditions, then the reduced action is a function of only r_+ and e , i.e. $I^* = I^*(r_+, e)$. The local stability conditions are then (i) $\nabla I^* = 0$ and (ii) the Hessian matrix is positive definite. The latter condition corresponds to a condition of dynamical as well as thermodynamical stability [10] and will be discussed in section V. We will start by investigating the first condition.

The condition of stationarity $\nabla I^* = 0$ gives

$$\beta = \frac{4\pi r_+^3}{r_+^2 - e^2 + 3\alpha^2 r_+^4} \sqrt{1 - \frac{r_+}{r_B} - \frac{e^2}{r_+ r_B} - \frac{\alpha^2 r_+^3}{r_B} + \frac{e^2}{r_B^2} + \alpha^2 r_B^2} \quad (33)$$

and

$$\phi = \left(\frac{e}{r_+} - \frac{e}{r_B} \right) \left(1 - \frac{r_+}{r_B} - \frac{e^2}{r_+ r_B} - \frac{\alpha^2 r_+^3}{r_B} + \frac{e^2}{r_B^2} + \alpha^2 r_B^2 \right)^{-1/2}. \quad (34)$$

These are the inverse Hawking temperature and the difference in the electrostatic potential between r_+ and r_B blueshifted from infinity to r_B , respectively.

Inverting these two equations, r_+ and e are obtained as functions of the boundary conditions and the cosmological constant. We define the more convenient variables

$$x \equiv \frac{r_+}{r_B}, \quad q \equiv \frac{e}{r_B}, \quad \bar{\beta} \equiv \frac{\beta}{4\pi r_B}, \quad \bar{\alpha}^2 \equiv \alpha^2 r_B^2. \quad (35)$$

In these variables (33) and (34) are written

$$\bar{\beta} = x \sqrt{1-x} \sqrt{1 - \frac{q^2}{x} + \bar{\alpha}^2 (1+x+x^2)} \left(1 - \frac{q^2}{x^2} + 3\bar{\alpha}^2 x^2 \right)^{-1}, \quad (36)$$

$$\phi = \frac{q}{x} \sqrt{1-x} \left(1 - \frac{q^2}{x} + \bar{\alpha}^2 (1+x+x^2) \right)^{-1/2}. \quad (37)$$

To invert this equations, we start by inverting equation (37) to obtain q ,

$$q^2 = x^2 \phi^2 [1 + \bar{\alpha}^2 (1+x+x^2)] (1-x+x\phi^2)^{-1}. \quad (38)$$

Substituting (38) in (36) and taking its square, we obtain a 7th degree equation in x with a double root $x = 1$ which is not a solution of the initial equations. Getting rid of that root, we obtain a 5th degree equation

$$\begin{aligned} \bar{\beta}^2 (-1 + \phi^2 + \bar{\alpha}^2 \phi^2)^2 + 4\bar{\alpha}^2 \bar{\beta}^2 \phi^2 (-1 + \phi^2 + \bar{\alpha}^2 \phi^2) x + (-1 - \bar{\alpha}^2 + 6\bar{\alpha}^2 \bar{\beta}^2 - 12\bar{\alpha}^2 \bar{\beta}^2 \phi^2 - \\ - 6\bar{\alpha}^4 \bar{\beta}^2 \phi^2 + 6\bar{\alpha}^2 \bar{\beta}^2 \phi^4 + 10\bar{\alpha}^4 \bar{\beta}^2 \phi^4) x^2 + (1 - \phi^2 - \bar{\alpha}^2 \phi^2 - 12\bar{\alpha}^4 \bar{\beta}^2 \phi^2 + 12\bar{\alpha}^4 \bar{\beta}^2 \phi^4) x^3 + \\ + \bar{\alpha}^2 (9\bar{\alpha}^2 \bar{\beta}^2 - \phi^2 - 18\bar{\alpha}^2 \bar{\beta}^2 \phi^2 + 9\bar{\alpha}^2 \bar{\beta}^2 \phi^4) x^4 + \bar{\alpha}^2 (1 - \phi^2) x^5 = 0. \end{aligned} \quad (39)$$

However not every solution of this equation corresponds to a physical solution of a black hole. This is because the radius of the event horizon of the Reissner-Nordström-anti-de Sitter must obey the following condition

$$r_+^2 - e^2 + 3\alpha^2 r_+^4 \geq 0. \quad (40)$$

Where the equality defines the extremal Reissner-Nordström-anti-de Sitter black hole.

Comparing (40) with (33), yields that β is real and positive. Comparing it with (34) we obtain the following condition

$$\phi^2 \leq \frac{1 + 3\alpha^2 r_+^2}{1 + \alpha^2 (1 + 2r_+ r_B + 3r_+^2)}. \quad (41)$$

In the coordinates given in (35), the inequality (41) becomes

$$\phi^2 \leq \frac{1 + 3\bar{\alpha}^2 x^2}{1 + \bar{\alpha}^2 (1 + 2x + 3x^2)}. \quad (42)$$

This is the condition that the solutions of equation (39) must obey in order to represent physical black hole solutions.

Equation (39) has no known analytical solutions. However its solutions can be numerically computed and presented in graphics. This will be done in the next section.

IV. ANALYSIS OF THE BLACK HOLE SOLUTIONS

In this section we present in graphics an analysis of the solutions of equation (39) that obey condition (42). This analysis is done in two steps: (i) first, we analyze figures 1 to 18, that present the solutions x as functions of $\bar{\beta}$ and

ϕ , for values $\bar{\alpha} = 0, 0.25, 0.5, 0.75, 1, 2.5, 5$ and 10 ; (ii) afterwards we show in figures 19 to 29 the regions with zero, one and two solutions in the space spanned by $\phi \times \bar{\alpha}$ for fixed values of $\bar{\beta}$.

(i) Analysis of figures 1 to 18:

$\bar{\alpha} = 0$: The solutions for $\bar{\alpha} = 0$ are presented in figures 1 and 2. These are obviously identical to the solutions of the Reissner-Nordström black hole, see [10]. We can see in figure 1 that for fixed ϕ there is a maximum of $\bar{\beta}$, $\bar{\beta}_{\max}(\phi)$, so that for $\bar{\beta} > \bar{\beta}_{\max}(\phi)$ there are no solutions. For $\bar{\beta} < \bar{\beta}_{\max}(\phi)$ one can have two or only one solution depending on the precise value of $\bar{\beta}$. For $\phi = 0$ (Schwarzschild) one has always two solutions for $\bar{\beta} < \bar{\beta}_{\max}(0)$ ($\bar{\beta}_{\max}(0) = 2/\sqrt{27}$). In the limiting case $\bar{\beta} \rightarrow 0$ (i.e. $r_B T \rightarrow \infty$), one finds there is a solution with $x = r_+/r_B \rightarrow 1$ (as will be seen in section V this is the stable solution), see [5]. For $\phi = 0$, still, and $\bar{\beta} > \bar{\beta}_{\max}(0)$ there are no solutions (see comments at the end of this section). For $0 < \phi < 1/\sqrt{3}$ one has one or two solutions up to $\bar{\beta}_{\max}(\phi)$, whereas for $\bar{\beta} > \bar{\beta}_{\max}(\phi)$ there are as well no solutions. Finally for $\phi > 1/\sqrt{3}$ there is only one solution (again for $\bar{\beta} < \bar{\beta}_{\max}(\phi)$) corresponding to the unstable branch as will be seen in section V. Note that, for $\bar{\alpha} = 0$, condition (42) implies that the electrostatic potential has a maximum at $\phi_{\max} = 1$ (see figure 2). Notice also that in the limit $\bar{\beta} \rightarrow \infty$ ($T \rightarrow 0$), the curves in figure 2 tend to the curve $\phi = 1$, which corresponds to the extremal Reissner-Nordström black hole ($r_+ = e$).

The cases $\bar{\alpha} \neq 0$, which are now going to be analyzed require the following prior analysis.

As in the case $\bar{\alpha} = 0$, for $\bar{\alpha} \neq 0$ there are solutions at $T = 0$ ($\bar{\beta} = \infty$), that correspond to the extremal black holes. This can be analytically verified by replacing $\bar{\beta} = \infty$ in equation (39), from where we obtain the equation

$$1 - \phi^2 - \bar{\alpha}^2 \phi^2 - 2\bar{\alpha}^2 \phi^2 x + 3\bar{\alpha}^2 (1 - \phi^2) x^2 = 0. \quad (43)$$

Notice this is the equation one obtains taking the equality in condition (42). In fact it corresponds to the condition of extremality of the Reissner-Nordström-anti-de Sitter black hole, which is in agreement with the well known fact that only the extremal black holes have zero temperature.

Equation (43) has at least one solution that verifies $0 < x < 1$ if

$$\begin{aligned} \bar{\alpha}^2 < \frac{1}{6} \quad \text{and} \quad \frac{1 + 3\bar{\alpha}^2}{1 + 6\bar{\alpha}^2} \leq \phi^2 \leq \frac{1}{1 + \bar{\alpha}^2}, \\ \frac{1}{6} \leq \bar{\alpha}^2 < \frac{2}{3} \quad \text{and} \quad \frac{3\bar{\alpha}^2 + 6 - \sqrt{9\bar{\alpha}^4 + 12\bar{\alpha}^2}}{4\bar{\alpha}^2 + 6} \leq \phi^2 \leq \frac{1}{1 + \bar{\alpha}^2}, \\ \bar{\alpha}^2 \geq \frac{2}{3} \quad \text{and} \quad \frac{3\bar{\alpha}^2 + 6 - \sqrt{9\bar{\alpha}^4 + 12\bar{\alpha}^2}}{4\bar{\alpha}^2 + 6} \leq \phi^2 \leq \frac{1 + 3\bar{\alpha}^2}{1 + 6\bar{\alpha}^2}. \end{aligned} \quad (44)$$

For these values of ϕ and $\bar{\alpha}$, the curves for fixed ϕ presented in the figures reach infinite $\bar{\beta}$. Furthermore, equation (43) has two solutions if

$$\begin{aligned} 1/6 < \bar{\alpha}^2 < 2/3 \quad \text{and} \quad \frac{3\bar{\alpha}^2 + 6 - \sqrt{9\bar{\alpha}^4 + 12\bar{\alpha}^2}}{4\bar{\alpha}^2 + 6} < \phi^2 < \frac{1 + 3\bar{\alpha}^2}{1 + 6\bar{\alpha}^2}, \\ \bar{\alpha}^2 \geq 2/3 \quad \text{and} \quad \frac{3\bar{\alpha}^2 + 6 - \sqrt{9\bar{\alpha}^4 + 12\bar{\alpha}^2}}{4\bar{\alpha}^2 + 6} < \phi^2 < \frac{1}{1 + \bar{\alpha}^2}. \end{aligned} \quad (45)$$

$\bar{\alpha} = 0.25$: The solutions for $\bar{\alpha} = 0.25$ are presented in figures 3 and 4. These figures present the same properties mentioned previously for the case $\bar{\alpha} = 0$. Comparing 1 and 3, we verify that the maximum value of $\bar{\beta}$, $\bar{\beta}_{\max}(\phi)$, for which there are solutions is increasing, i.e. there are solutions for slightly lower values of the temperature at $\bar{\alpha} = 0.25$ than at $\bar{\alpha} = 0$. The curves for $\phi = 0, 0.5, 0.7, 0.9$ in figure 3 have solutions only for $\bar{\beta} < \bar{\beta}_{\max}(\phi)$. However the curve $\phi = 0.95$ goes to infinity. It can be seen from (44) that the curves that go to infinity have $0.93 \lesssim \phi \lesssim 0.97$.

Condition (42) implies, for $\bar{\alpha}^2 < 2/3$,

$$\phi \leq \sqrt{\frac{1}{1 + \bar{\alpha}^2}}. \quad (46)$$

This condition corresponds to the upper-limit of the interval given in (44), which in this case is $\phi \simeq 0.97$. Notice that if in equation (39) we do $x = 0$, we obtain precisely $\phi = 1/\sqrt{1 + \bar{\alpha}^2}$, as can be seen in figure 4.

$\bar{\alpha} = 0.5$: The solutions for $\bar{\alpha} = 0.5$ are presented in figures 5 and 6. The properties mentioned previously still hold for $\bar{\alpha} = 0.5$. There are solution for infinite $\bar{\beta}$ in the interval $0.83 \lesssim \phi \lesssim 0.89$, see (44), as an example the curve for $\phi = 0.85$ is presented in figure 5. From condition (46), we have $\phi \lesssim 0.89$, this can be seen in figure 6 and it is the reason why the curve $\phi = 0.9$ no longer appears in figure 5.

$\bar{\alpha} = 0.75$: The solutions for $\bar{\alpha} = 0.75$ are presented in figures 7 to 9. As mentioned above, the values of $\bar{\beta}$ for which solutions can be found are increasing, as can be seen in figure 7 comparing it with other figures with lower values of $\bar{\alpha}$. In figure 8 the curves $\phi = 0.75, 0.77$ reach infinity, using (45) we can verify that curves with $0.75 \lesssim \phi \lesssim 0.78$ reach infinite $\bar{\beta}$. In figure 9 we can see that $\phi < 0.8$, which can also be inferred from (46).

$\bar{\alpha} = 1$: Figures 10 and 11 plot the solutions for $\bar{\alpha} = 1$. We can see that this figures present similar properties to the ones obtained for lower values of $\bar{\alpha}$. Using (44), we can see that for $\phi \lesssim 0.66$ there are solutions only for $\bar{\beta} < \bar{\beta}_{\max}(\phi)$, where $\bar{\beta}_{\max}(\phi)$ is finite and depends on ϕ . On the contrary, the curves for higher values of ϕ reach infinite $\bar{\beta}$. In particular, for $0.66 \lesssim \phi \lesssim 0.71$ (see equation (45)) there are two solutions at low temperatures (i.e., high $\bar{\beta}$) as can be seen in curve $\phi = 0.7$ in figure 10. This can also be seen in figure 11, since the curve $\bar{\beta} = 9$ is representative of the curves with high $\bar{\beta}$. It can be seen that for $\bar{\beta} = 9$ there are two solutions for $\phi < \phi_0$, where $\phi_0 = \frac{1}{\sqrt{1+\bar{\alpha}^2}} \simeq 0.71$ is the value of ϕ where $x = 0$ for every $\bar{\beta}$. There is one solution for $0.71 \lesssim \phi \lesssim 0.76$, see figure 11, where the upper-limit is imposed by condition (42). In fact, condition (42) imposes, for $\bar{\alpha}^2 < 2/3$,

$$\phi_{\max} = \sqrt{\frac{1 + 3\bar{\alpha}^2}{1 + 6\bar{\alpha}^2}}. \quad (47)$$

Notice this is the upper-limit of the interval given in (44).

$\bar{\alpha} = 2.5$: In figures 12 to 14 the solutions for $\bar{\alpha} = 2.5$ are plotted. In figure 12 we can see that for $\phi \lesssim 0.36$ (see also (44)) there are solutions only for $\bar{\beta} < \bar{\beta}_{\max}(\phi)$, where $\bar{\beta}_{\max}(\phi)$ is a certain finite value of $\bar{\beta}$ that depends on ϕ . Using (45), we see that for $0.364 \lesssim \phi \lesssim 0.371$ there are two solutions at high values of $\bar{\beta}$, see as an example curve $\phi = 0.37$ in figure 13, which reaches infinite $\bar{\beta}$. According to (44), for $0.37 \lesssim \phi \lesssim 0.72$ there is only one solution that reaches infinite $\bar{\beta}$, see curves $\phi = 0.5, 0.7$, in figure 12, and $\phi = 0.38$, in figure 13. In figure 14 we can see that for high values of $\bar{\beta}$, e.g. $\bar{\beta} = 9$, the interval of values of ϕ for which there are two solutions is very thin and is found precisely at slightly lower values than $\phi_0 = 1/\sqrt{1+\bar{\alpha}^2} \simeq 0.37$, which is in agreement with (45). For $\phi > \phi_0$ there is only one solution up to $\phi_{\max} \simeq 0.72$, see (47).

$\bar{\alpha} = 5$: Figures 15 and 16 present the solutions for $\bar{\alpha} = 5$. Using (44), we can see that for $\phi \lesssim 0.19$, there are solutions only for $\bar{\beta} < \bar{\beta}_{\max}(\phi)$, see curve $\phi = 0$ in figure 15. For $0.19 \lesssim \phi \lesssim 0.71$ there is one solution for high values of $\bar{\beta}$, see curves $\phi = 0.3, 0.5, 0.7$ in figure 15. These curves reach infinite $\bar{\beta}$. In figure 16, we can see that for high $\bar{\beta}$ (consider the curve $\bar{\beta} = 9$) there is a very thin region of values ϕ where there are two solutions. For infinite $\bar{\beta}$ this region is $0.195 \lesssim \phi \lesssim 0.196$, see (45). In figure 16, we can also see that for $0.19 \lesssim \phi \lesssim 0.71$ there is one solution, where the upper-limit is given by (47).

$\bar{\alpha} = 10$: Figures 17 and 18 present the solutions for $\bar{\alpha} = 10$. In these figures we can verify the same properties described for other values of $\bar{\alpha}$. According to (44), for $\phi \lesssim 0.099$ there are solutions only for $\bar{\beta} < \bar{\beta}_{\max}(\phi)$, see curve $\phi = 0$ in figure 17, see also figure 18. There is a very narrow interval for which there are two solutions at high values of $\bar{\beta}$, $0.0987 \lesssim \phi \lesssim 0.0995$, according to (45) (see curve $\bar{\beta} = 9$ in figure 18). For $0.0995 \lesssim \phi \lesssim 0.7077$ there is one solution for high values of $\bar{\beta}$, see curves $\phi = 0.3, 0.5, 0.7$ in figure 17 (this curves reach infinite $\bar{\beta}$) and figure 18.

For higher values of $\bar{\alpha}$ there are not new types of solutions and therefore it is not necessary to pursue our analysis.

(ii) Analysis of figures 19 to 29:

In order to clarify the disposition of the number of solutions for given values of $\bar{\alpha}$, ϕ , and $\bar{\beta}$, we present, in the space spanned by $\bar{\alpha}$ and ϕ for fixed $\bar{\beta}$, the regions with zero, one and two solutions. We do this for eleven different values of $\bar{\beta}$, $\bar{\beta} = 0, 0.01, 0.1, 0.3, 2/\sqrt{27} \simeq 0.38, 1, 2, 5, 10, 100, \infty$, see figures 19 to 29 respectively. In this figures one can see the evolution of the number of solutions as $\bar{\beta}$ increases. To present all possible values of $\bar{\alpha} \in [0, \infty[$, we use in these figures the parameter a instead of $\bar{\alpha}$, a is defined by

$$a = \frac{2}{\pi} \arctan \bar{\alpha}, \quad (48)$$

such that $0 \leq a \leq 1$. It is this variable that appears in the ordinate axis in figures 19 to 29.

Due to condition (42) there are no physically possible solutions on the right-hand side of figures 19 to 29.

An important value of $\bar{\beta}$, first studied by York [5] in connection with the Schwarzschild black hole ($\phi = \bar{\alpha} = 0$), is $\bar{\beta} = 2/\sqrt{27} \simeq 0.38$, i.e. $\beta = \frac{8\pi}{\sqrt{27}} r_B$. For higher values of β , lower values of the temperature, there are no black hole solutions. This is a quantum effect and following York [5] can be understood as follows. One can associate a Compton type wavelength λ to the energy $k_B T$ of the thermal particles, by $\lambda = \frac{hc}{k_B T}$, or in Planck units $\lambda = 1/T = \beta$. If this Compton wavelength is much larger than the radius r_B of the cavity (or more specifically $\lambda > \frac{8\pi}{\sqrt{27}} r_B \simeq 4.8 r_B$) then the thermal particles cannot be confined within the cavity and do not collapse to form a black hole.

By analyzing figures 22 and 23, we can see that for nonzero cosmological constant ($\bar{\alpha} \neq 0$) this phenomenon starts at even lower β (higher T). Indeed using equation (36) (with $\phi = 0$, i.e. $q = 0$) we can show that to first order in α^2 ($\alpha^2 r_B^2 \ll 1$), York's criterion for no black hole solutions becomes

$$\lambda = \beta > \frac{8\pi}{\sqrt{27}} r_B \left(1 - \frac{5}{18} \alpha^2 r_B^2 \right). \quad (49)$$

From equation (49) we infer that the role of the negative cosmological constant ($\Lambda = -3\alpha^2$) is to produce an effective cavity radius $r_{\text{eff}} = r_B \left(1 - \frac{5}{18} \alpha^2 r_B^2 \right)$ smaller than r_B . Thus for a given temperature, it is more difficult to confine the thermal particles, and harder to form black holes, in accord with the idea that a negative cosmological constant shrinks space.

If we extend our previous first order analysis to include the electrostatic potential ϕ , we obtain

$$\lambda = \beta > \frac{8\pi}{\sqrt{27}} r_B \left(1 - \frac{5}{18} \alpha^2 r_B^2 + 2\phi^2 \right). \quad (50)$$

We can see that the electrostatic potential has the opposite effect of the cosmological constant (see for example figures 22, 23 and 24).

V. STABILITY

As mentioned before there is a second condition of local stability that has not yet been investigated. We will follow the same procedure as given in [10]. This is the condition that the Hessian matrix of the reduced action be positive definite. For convenience in this analysis we will use the variable $S = \pi r_+^2$ instead r_+ . The Hessian matrix of $I^*(S, e)$ is

$$I_{,ij}^* = \begin{pmatrix} I_{,ee}^* & I_{,eS}^* \\ I_{,eS}^* & I_{,SS}^* \end{pmatrix}. \quad (51)$$

The matrix is positive definite if its pivots are all positive. The pivots of (51) are

$$I_{,ee}^* \quad (52)$$

and

$$\frac{\det(I_{,ij}^*)}{I_{,ee}^*}. \quad (53)$$

The first condition of local stability, $\nabla I^* = 0$ yields

$$\begin{aligned} \left(\frac{\partial I^*}{\partial e} \right)_S &= \beta \left(\frac{\partial E^*}{\partial e} \right)_S - \beta \phi = 0 \quad \Rightarrow \quad \phi = \left(\frac{\partial E}{\partial e} \right)_S, \\ \left(\frac{\partial I^*}{\partial S} \right)_e &= \beta \left(\frac{\partial E^*}{\partial S} \right)_e - 1 = 0 \quad \Rightarrow \quad \beta^{-1} = T = \left(\frac{\partial E}{\partial S} \right)_e. \end{aligned} \quad (54)$$

These are well known thermodynamical relations [15]. From (54), we compute the second derivatives of I^* in the stationary points of I^*

$$\begin{aligned} \left. \frac{\partial^2 I^*}{\partial e^2} \right|_{\text{eq}} &= \beta \left. \frac{\partial^2 E^*}{\partial e^2} \right|_{\text{eq}} = \beta \left(\frac{\partial \phi}{\partial e} \right)_S \\ \left. \frac{\partial^2 I^*}{\partial e \partial S} \right|_{\text{eq}} &= \beta \left. \frac{\partial^2 E^*}{\partial e \partial S} \right|_{\text{eq}} = \beta \left(\frac{\partial \phi}{\partial S} \right)_e = -\frac{1}{\beta} \left(\frac{\partial \beta}{\partial e} \right)_S \\ \left. \frac{\partial^2 I^*}{\partial S^2} \right|_{\text{eq}} &= \beta \left. \frac{\partial^2 E^*}{\partial S^2} \right|_{\text{eq}} = -\frac{1}{\beta} \left(\frac{\partial \beta}{\partial S} \right)_e. \end{aligned} \quad (55)$$

where eq means quantities evaluated at equilibrium, i.e. at the stationary points of the reduced action I^* .

The first pivot (52) is simply the first of these equations. The second pivot (53) is easily obtained from (55)

$$\begin{aligned}
\frac{\det I_{,ij}^*}{I_{,ee}^*} &= -\frac{1}{\beta} \left(\frac{\partial \beta}{\partial S} \right)_e + \frac{1}{\beta} \left(\frac{\partial \beta}{\partial e} \right)_S \left(\frac{\partial \phi}{\partial S} \right)_e / \left(\frac{\partial \phi}{\partial e} \right)_S \\
&= -\frac{1}{\beta} \left[\left(\frac{\partial \beta}{\partial S} \right)_e + \left(\frac{\partial \beta}{\partial e} \right)_S \left(\frac{\partial e}{\partial S} \right)_\phi \right] \\
&= -\frac{1}{\beta} \left(\frac{\partial \beta}{\partial S} \right)_\phi = \frac{1}{C_{\phi, r_B}},
\end{aligned} \tag{56}$$

where C_{ϕ, r_B} is the heat capacity at constant ϕ and r_B . Notice that in all this calculation we have implicitly held r_B constant, since in the grand canonical ensemble the dimension of the system is held constant.

Imposing positive pivots for local stability yields

$$\begin{aligned}
\left(\frac{\partial \phi}{\partial e} \right)_{S, r_B} &\geq 0, \\
C_{\phi, r_B} &\geq 0.
\end{aligned} \tag{57}$$

These conditions are identical to the classical thermodynamical stability conditions [15]. Therefore one can conclude that the dynamical stability conditions given in (54) and (57) are identical to the thermodynamical stability conditions [10].

For the Reissner-Nordström-anti-de Sitter black hole, the pivots obtained from (55) and (56) are

$$\begin{aligned}
\left(\frac{\partial \phi}{\partial e} \right)_{S, r_B} &= \left(\frac{1}{r_+} - \frac{1}{r_B} \right) \left(1 - \frac{r_+}{r_B} - \frac{e^2}{r_+ r_B} - \frac{\alpha^2 r_+^3}{r_B} + \frac{e^2}{r_B^2} + \alpha^2 r_B^2 \right)^{1/2} + \\
&\quad + \frac{e^2}{r_B} \left(\frac{1}{r_+} - \frac{1}{r_B} \right)^2 \left(1 - \frac{r_+}{r_B} - \frac{e^2}{r_+ r_B} - \frac{\alpha^2 r_+^3}{r_B} + \frac{e^2}{r_B^2} + \alpha^2 r_B^2 \right)^{3/2},
\end{aligned} \tag{58}$$

which is positive, and

$$\begin{aligned}
C_{\phi, r_B} &= 4\pi r_+^3 (r - r_+) (r_+^2 - e^2 + 3\alpha^2 r_+^4) [1 + \alpha^2 (r_B^2 + r_+ r_B + r_+^2)] \times \\
&\quad \times \{ e^4 + r_+^3 [(6\alpha^2 r_+^2 - 2)(r_B + \alpha^2 r_B^3) + 3r_+ + 2\alpha^2 r_+^3 + 3\alpha^4 r_+^5] + \\
&\quad + 2e^2 r_+ [-2r_+ + r_B (1 + \alpha^2 (r_B^2 - 2r_+ r_B - 2r_+^2))] \}^{-1}.
\end{aligned} \tag{59}$$

The numerator of C_{ϕ, r_B} is positive, therefore the condition $C_{\phi, r_B} > 0$ is verified if the denominator in (59) is positive. Using (35) and (38), we obtain the following condition of stability for the solutions of equation (39)

$$\begin{aligned}
&[-2(1 + \bar{\alpha}^2) + 3x + 6\bar{\alpha}^2(1 + \bar{\alpha}^2)x^2 + 2\bar{\alpha}^2 x^3 + 3\bar{\alpha}^4 x^5] (1 - x + x\phi^2)^2 - \\
&- [2\phi^2(1 + \bar{\alpha}^2(1 + x + x^2))(-1 + 2x + \bar{\alpha}^2(-1 + 2x + 2x^2))] (1 - x + x\phi^2) + \\
&+ \phi^4 x (1 + \bar{\alpha}^2(1 + x + x^2))^2 > 0.
\end{aligned} \tag{60}$$

By numerical computation, we can verify the solutions that obey this condition.

As an example the stable solutions for $\bar{\alpha} = 1$ and $\bar{\alpha} = 5$ are presented in figures 30 and 31. Comparing these figures with figures 10 and 15 respectively, we can easily distinguish the stable and unstable solutions, i.e. the solutions that verify or not equation (60).

Analyzing figures 30 and 31, we can see that in general only the solutions with the higher value of x , that is with higher event horizon radius, are stable. In more detail we can distinguish three cases: (i) for curves with fixed ϕ , that depart from $\bar{\beta} = 0$ and for relatively low values of $\bar{\beta}$ where there is a single solution, this solution is unstable (e.g. $\phi = 0.5, 0.6$ in figures 10 and 30); (ii) whenever there are two solutions, for given values of $\bar{\beta}, \phi, \bar{\alpha}$, the smaller one is an instanton (i.e. it is an unstable solution and dominates the semi-classical evaluation of the rate of nucleation of black holes [21]) and the one with larger event horizon radius is a stable black hole (e.g. $\phi = 0, 0.5, 0.6, 0.7$ in figures 10 and 30 and $\phi = 0$ in curves 15 and 31); (iii) for curves with fixed ϕ , that reach infinite $\bar{\beta}$ and that correspond to a single solution, this solution is stable (e.g. $\phi = 0.3, 0.5, 0.7$ in figures 15 and 31).

These three cases can easily be distinguished in figures 19 to 29. In these figures there are in general two separated regions with one solution. The region with lower values of a , i.e. lower values of $\bar{\alpha}$, corresponds to case (i) and these are unstable solutions. The region with higher values of a corresponds to case (iii) and these are stable solutions. Obviously, the region with two solutions in each figure 19 to 29, corresponds to case (ii), i.e. one of those solution is stable, the one with higher value of x , and the other unstable.

VI. COMMENTS ON SPECIAL CASES

Several black holes may be considered as special cases of the Reissner-Nordström-anti-de Sitter black hole.

- (I) putting $\phi = 0$ and $\Lambda = 0$, we obtain the Schwarzschild black hole studied in [5]. There are two solutions for $\bar{\beta} < \bar{\beta}_{\max} = 2/\sqrt{27}$. This solutions can be computed analytically, since equation (39) becomes a 3rd degree equation for $\Lambda = 0$. Only the solution with higher event horizon radius, i.e. higher mass, is stable.
- (II) putting $\Lambda = 0$ we obtain the Reissner-Nordström black hole. This has been studied by [10]. There are one or two solution for $\bar{\beta} < \bar{\beta}_{\max}$. These as stated above can be computed analytically. Once again only the solution with higher event horizon radius, when it exists, is stable.
- (III) putting $\phi = 0$ we obtain the Schwarzschild-anti-de Sitter. This black hole as been studied before, see [16,11]. This black hole has two solutions for $\beta < \beta_{\max}$, and again only the one with higher event horizon radius is stable [11].
- (IV) the extremal cases require special care [22–24] and were not studied in any detail in this paper.

VII. CONCLUSIONS

We have studied the thermodynamics of the Reissner-Nordström-anti-de Sitter black hole in York's formalism. In the grand canonical ensemble where the temperature and the electrostatic potential are fixed at a boundary with finite radius, we have found one or two black hole solutions depending on the boundary conditions and the value of the cosmological constant. In general when there are two solutions, one is stable, the one with larger event horizon radius, and the other is an instanton. On the other hand, the cases with a single solution can correspond either to a stable or unstable solution. We have found that both high values of the cosmological constant and low temperatures favor stable solutions.

ACKNOWLEDGMENTS

C.S.P. acknowledges a research grant from JNICT FMRH/BIC/1535/95.

-
- [1] J. B. Hartle and S. W. Hawking, Phys. Rev. D **13**, 2188 (1976).
 - [2] G. W. Gibbons and S. W. Hawking, Phys. Rev. D **15**, 2752 (1977).
 - [3] S. W. Hawking, in *General Relativity: An Einstein Centenary Survey*, edited by S. W. Hawking and W. Israel (Cambridge University Press, Cambridge, 1979).
 - [4] S. W. Hawking, Phys. Rev. D **13**, 191 (1976).
 - [5] J. W. York, Phys. Rev. D **33**, 2091 (1986).
 - [6] B. F. Whiting and J. W. York, Phys. Rev. Lett. **61**, 1336 (1988).
 - [7] B. F. Whiting, Class. Quantum Grav. **7**, 15 (1990).
 - [8] J. D. Brown and J. W. York, in *The Black Hole 25 Years After*, edited by C. Teitelboim and J. Zanelli (Plenum, New York, in press), gr-qc/9405024.
 - [9] J. D. Brown *et al.*, Class. Quantum Grav. **7**, 1433 (1990).
 - [10] H. W. Braden, J. D. Brown, B. F. Whiting, and J. W. York, Phys. Rev. D **42**, 3376 (1990).
 - [11] J. D. Brown, J. Creighton, and R. B. Mann, Phys. Rev. D **50**, 6394 (1994).
 - [12] J. Louko and S. N. Winters-Hilt, Phys. Rev. D **54**, 2647 (1996).
 - [13] J. P. S. Lemos, Phys. Rev. D **54**, 6206 (1996).
 - [14] J. W. York, Physica A **158**, 425 (1989).
 - [15] H. B. Callen, *Thermodynamics and an Introduction to Thermostatistics* (John Wiley & Sons, New York, 1985).
 - [16] S. W. Hawking and D. N. Page, Commun. Math. Phys. **87**, 577 (1983).
 - [17] D. N. Page, in *Black Hole Physics*, edited by V. D. Sabbata and Z. Zhang (Kluwer Academic, Dordrecht, 1992).
 - [18] S. W. Hawking, Commun. Math. Phys. **43**, 199 (1975).

- [19] J. D. Bekenstein, Phys. Rev. D **7**, 2333 (1973).
- [20] G. W. Gibbons and S. W. Hawking, Commun. Math. Phys. **66**, 291 (1979).
- [21] D. J. Gross, M. J. Perry and L. G. Yaffe, Phys. Rev. D **25**, 330 (1982).
- [22] S. W. Hawking, G. T. Horowitz, and S. F. Ross, Phys. Rev. D **51**, 4302 (1995).
- [23] O. B. Zaslavskii, Phys. Rev. Lett. **76**, 2211 (1996).
- [24] A. Ghosh and P. Mitra, Phys. Rev. Lett. **78**, 1858 (1997).

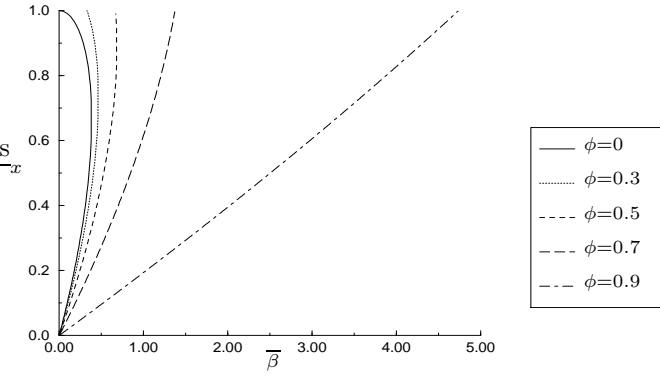


FIG. 1. Solutions of equation (39) for $\bar{\alpha} = 0$ (Reissner-Nordström) as a function of the variable $\bar{\beta}$ for fixed values of the electrostatic potential at the boundary $\phi = 0, 0.3, 0.5, 0.7, 0.9$. For each value of ϕ there is a value $\bar{\beta}_{\max}(\phi)$, so that only for $\bar{\beta} < \bar{\beta}_{\max}(\phi)$ there are solutions.

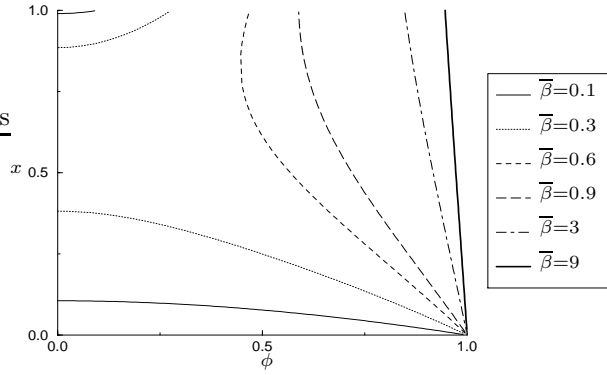


FIG. 2. Solutions of equation (39) for $\bar{\alpha} = 0$ (Reissner-Nordström) as a function of the electrostatic potential at the boundary ϕ for fixed values of $\bar{\beta} = 0.1, 0.3, 0.6, 0.9, 3, 9$.

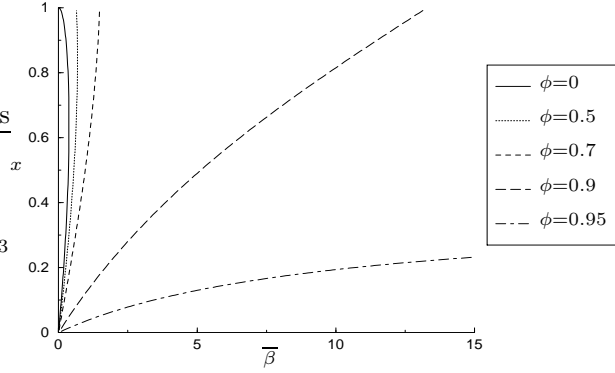


FIG. 3. Solutions of equation (39) for $\bar{\alpha} = 0.25$ as a function of the variable $\bar{\beta}$ for fixed values of the electrostatic potential at the boundary $\phi = 0, 0.5, 0.7, 0.9, 0.95$. The solutions for $\bar{\alpha} = 0.25$ are very similar to the solutions for $\bar{\alpha} = 0$ (see figure 1). However the curve $\phi = 0.95$ reaches infinite $\bar{\beta}$.

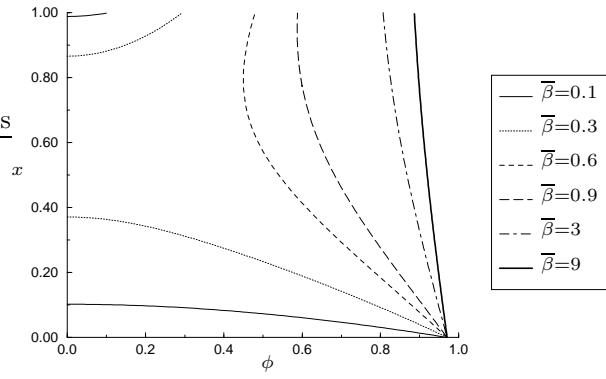


FIG. 4. Solutions of equation (39) for $\bar{\alpha} = 0.25$ as a function of the electrostatic potential at the boundary ϕ for fixed values of $\bar{\beta} = 0.1, 0.3, 0.6, 0.9, 3, 9$. Notice that $\phi \lesssim 0.97$ due to condition (42).

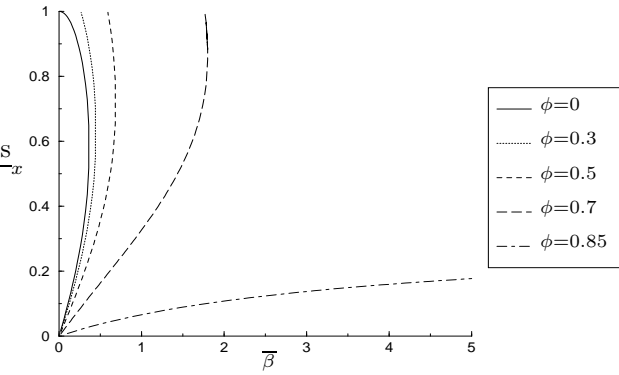


FIG. 5. Solutions of equation (39) for $\bar{\alpha} = 0.5$ as a function of the variable $\bar{\beta}$ for fixed values of the electrostatic potential at the boundary $\phi = 0, 0.3, 0.5, 0.7, 0.85$. For $\bar{\alpha} = 0.5$, due to condition (42), we have $\phi \lesssim 0.89$, consequently for $\phi = 0.9$ there are no solutions, this is why this curve is not presented. Curve $\phi = 0.85$ reaches infinite $\bar{\beta}$.

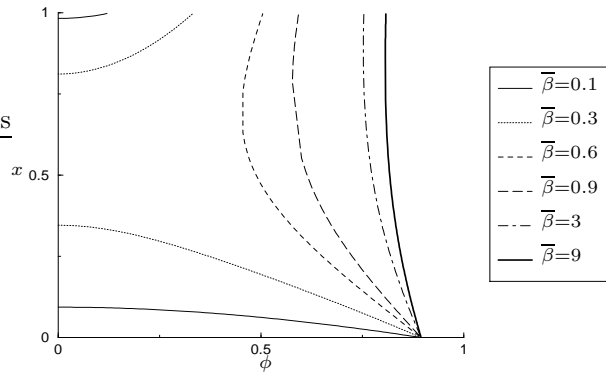


FIG. 6. Solutions of equation (39) for $\bar{\alpha} = 0.5$ as a function of the electrostatic potential at the boundary ϕ for fixed values of $\bar{\beta} = 0.1, 0.3, 0.6, 0.9, 3, 9$. Notice that $\phi \lesssim .89$, as imposed by condition (42).

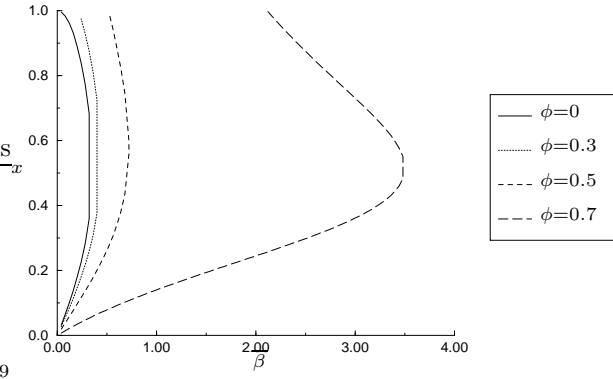


FIG. 7. Solutions of equation (39) for $\bar{\alpha} = 0.75$ as a function of the variable $\bar{\beta}$ for fixed values of the electrostatic potential at the boundary $\phi = 0, 0.3, 0.5, 0.7$. This figure is quite similar to the previous ones. However, for example the curve $\phi = 0.7$ reaches higher values of $\bar{\beta}$ and also for relatively high values of $\bar{\beta}$ ($2 \lesssim \bar{\beta} \lesssim 4$) there are two solutions.

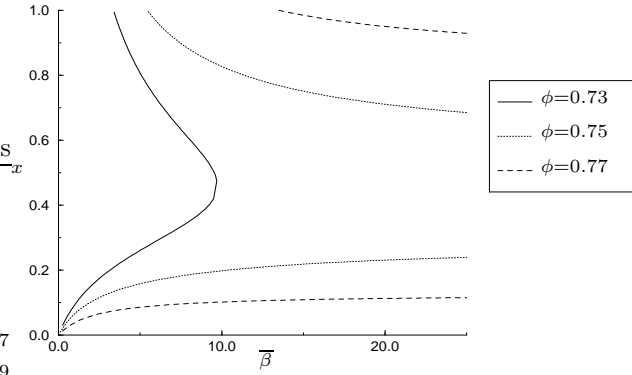


FIG. 8. Solutions of equation (39) for $\bar{\alpha} = 0.75$ as a function of the variable $\bar{\beta}$ for fixed values of the electrostatic potential at the boundary $\phi = 0.73, 0.75, 0.77$. Curves corresponding to $\phi = 0.75, 0.77$ reach infinite $\bar{\beta}$.

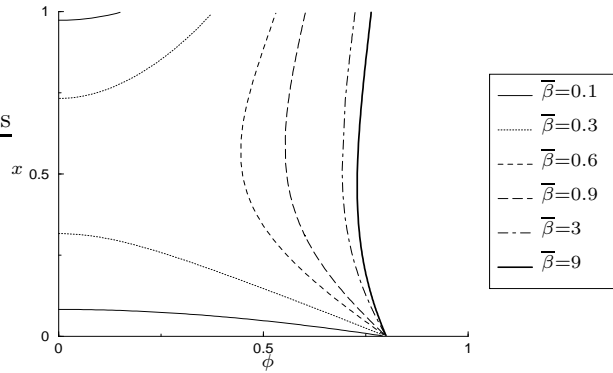


FIG. 9. Solutions of equation (39) for $\bar{\alpha} = 0.75$ as a function of the electrostatic potential at the boundary ϕ for fixed values of $\bar{\beta} = 0.1, 0.3, 0.6, 0.9, 3, 9$. The point where all curves join at $x = 0$ and which is the higher value of ϕ is $\phi_{\max} = .8$, imposed by condition (42).

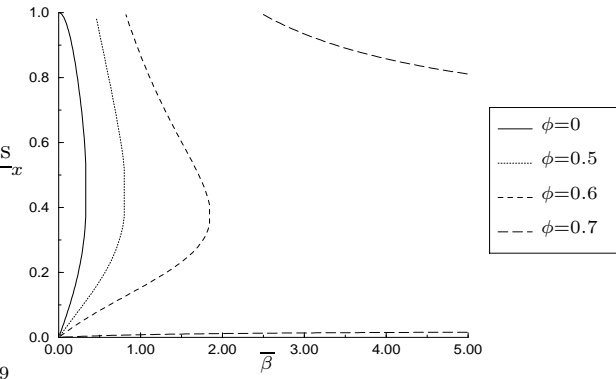


FIG. 10. Solutions of equation (39) for $\bar{\alpha} = 1$ as a function of the variable $\bar{\beta}$ for fixed values of the electrostatic potential at the boundary $\phi = 0, 0.5, 0.7$. For $\phi = 0.7$, there are two solutions that reach infinite $\bar{\beta}$.

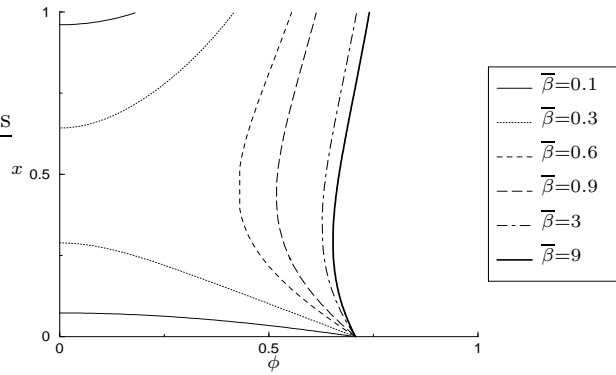


FIG. 11. Solutions of equation (39) for $\bar{\alpha} = 1$ as a function of the electrostatic potential at the boundary ϕ for fixed values of $\bar{\beta} = 0.1, 0.3, 0.6, 0.9, 3, 9$. The maximum value of ϕ for which there are solutions, $\phi_{\max} \simeq 0.76$ is imposed by condition (42).

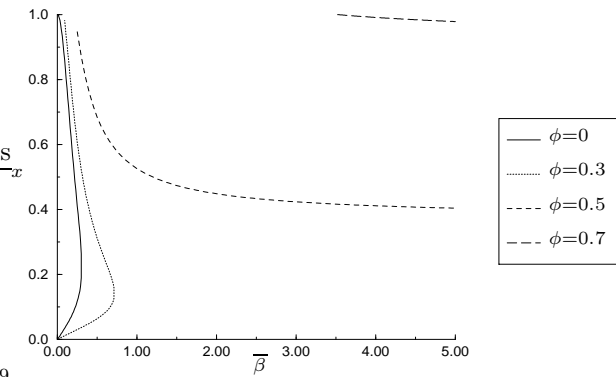


FIG. 12. Solutions of equation (39) for $\bar{\alpha} = 2.5$ as a function of the variable $\bar{\beta}$ for fixed values of the electrostatic potential at the boundary $\phi = 0, 0.3, 0.5, 0.7$. The curves $\phi = 0.5, 0.7$ reach infinite $\bar{\beta}$.

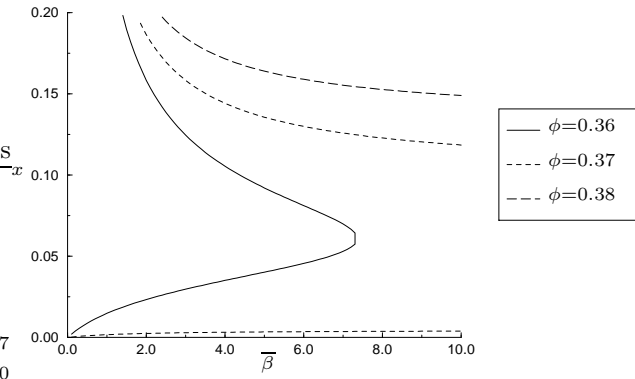


FIG. 13. Solutions of equation (39) for $\bar{\alpha} = 2.5$ as a function of the variable $\bar{\beta}$ for fixed values of the electrostatic potential at the boundary $\phi = 0.36, 0.37, 0.38$. The curves $\phi = 0.37, 0.38$ reach infinite $\bar{\beta}$.

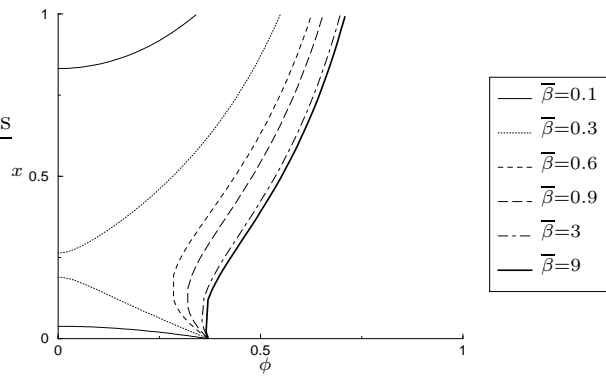


FIG. 14. Solutions of equation (39) for $\bar{\alpha} = 2.5$ as a function of the electrostatic potential at the boundary ϕ for fixed values of $\bar{\beta} = 0.1, 0.3, 0.6, 0.9, 3, 9$. There are solutions only for $\phi \lesssim 0.75$, due to condition (42).

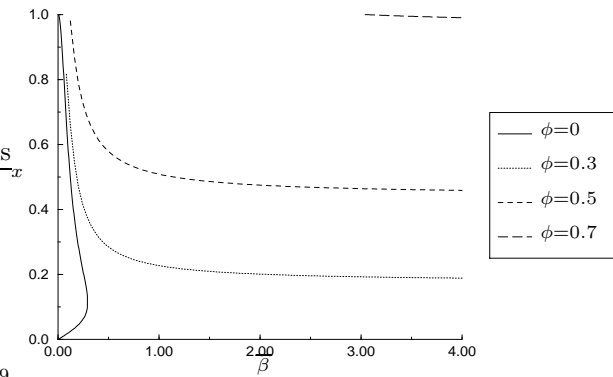


FIG. 15. Solutions of equation (39) for $\bar{\alpha} = 5$ as a function of the variable $\bar{\beta}$ for fixed values of the electrostatic potential at the boundary $\phi = 0, 0.3, 0.5, 0.7$. The curves $\phi = 0.3, 0.5$ e 0.7 reach infinity.

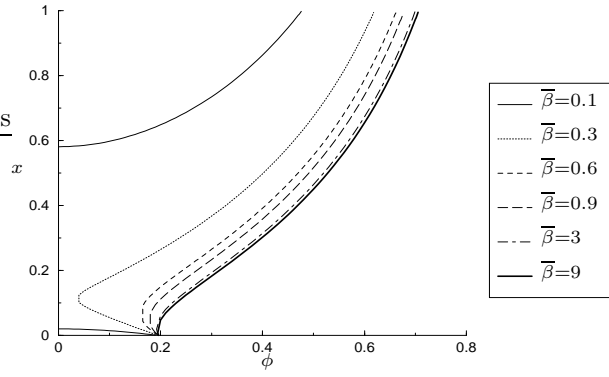


FIG. 16. Solutions of equation (39) for $\bar{\alpha} = 5$ as a function of the electrostatic potential at the boundary ϕ for fixed values of $\bar{\beta} = 0.1, 0.3, 0.6, 0.9, 3, 9$. The maximum value of ϕ for which there are solutions, $\phi_{\max} \simeq 0.71$, is imposed by condition (42).

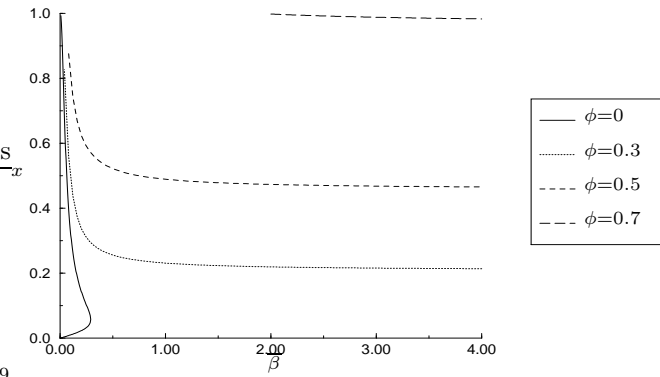


FIG. 17. Solutions of equation (39) for $\bar{\alpha} = 10$ as a function of the variable $\bar{\beta}$ for fixed values of the electrostatic potential at the boundary $\phi = 0, 0.3, 0.5, 0.7$. The curves $\phi = 0.3, 0.5, 0.7$ reach infinity.

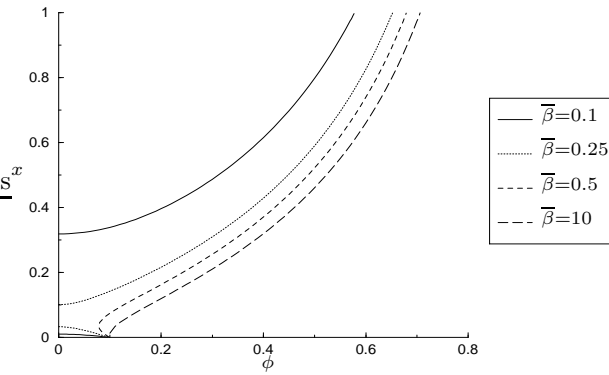


FIG. 18. Solutions of equation (39) for $\bar{\alpha} = 10$ as a function of the electrostatic potential at the boundary ϕ for fixed values of $\bar{\beta} = 0.1, 0.25, 0.5, 10$. The maximum value of ϕ for which there are solutions $\phi_{\max} \simeq 0.71$ is imposed by condition (42).

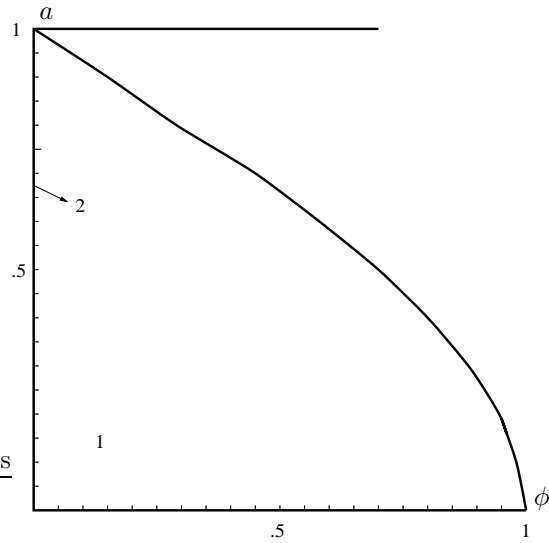


FIG. 19. Number of solutions of equation (39) with $\bar{\beta} \rightarrow 0$, in the space $\phi \times a$, where a is given by equation (48). There is one black hole solution in the confined region and also for $a = 1$ (i.e. infinite cosmological constant), for $\phi < \sqrt{0.5}$. There are two solutions for $\phi = 0$, i.e. for the Schwarzschild-anti-de Sitter black hole.

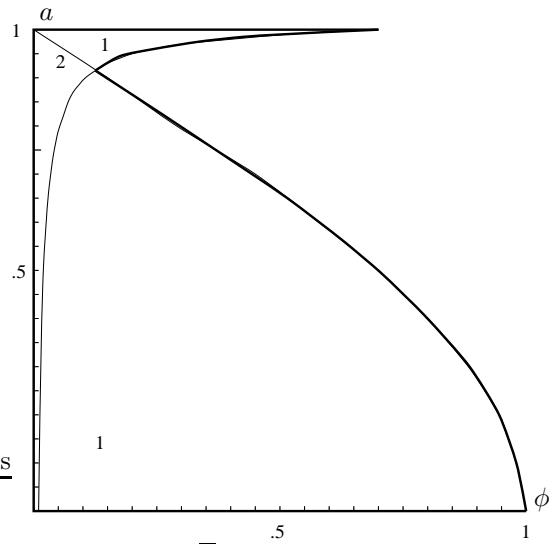


FIG. 20. Number of solutions of equation (39) with $\bar{\beta} = 0.01$, in the space $\phi \times a$, where a is given by equation (48). 0 - means that there are zero solutions in this region, i.e. there are no solutions of black holes in thermodynamical equilibrium for this set of values of $\bar{\beta}$, ϕ and a . 1 - means that there is one solution. 2 - means that there are two solutions.

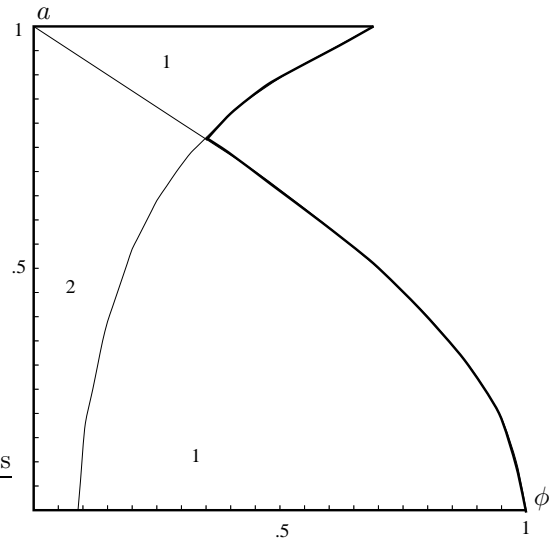


FIG. 21. Number of solutions of equation (39) with $\bar{\beta} = 0.1$, in the space $\phi \times a$, where a is given by equation (48) (see caption of figure 20).

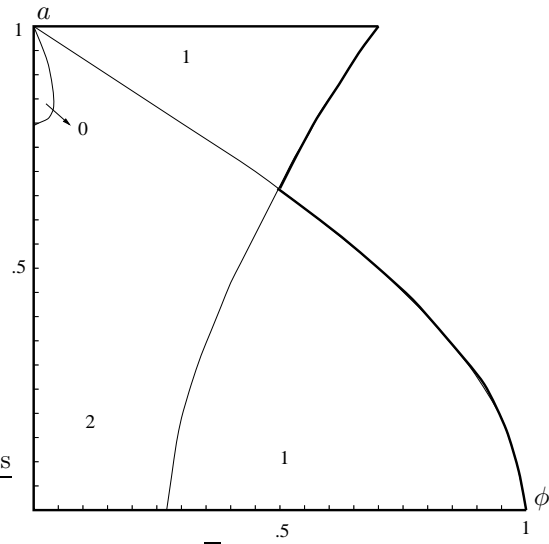


FIG. 22. Number of solutions of equation (39) with $\bar{\beta} = 0.3$, in the space $\phi \times a$, where a is given by equation (48) (see caption of figure 20).

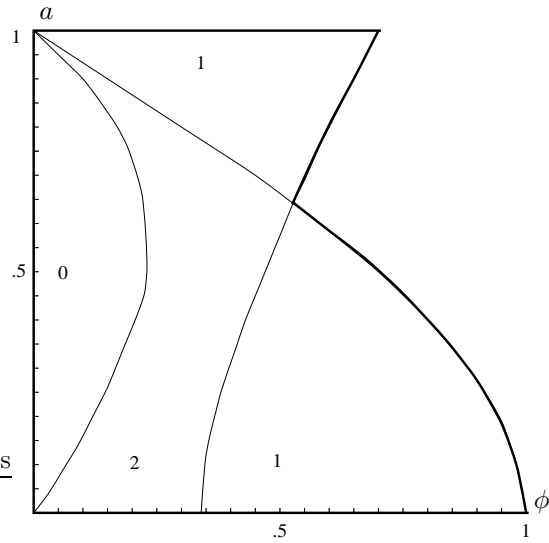


FIG. 23. Number of solutions of equation (39) with $\bar{\beta} = \frac{2}{\sqrt{27}} \simeq 0.38$, in the space $\phi \times a$, where a is given by equation (48) (see caption of figure 20).

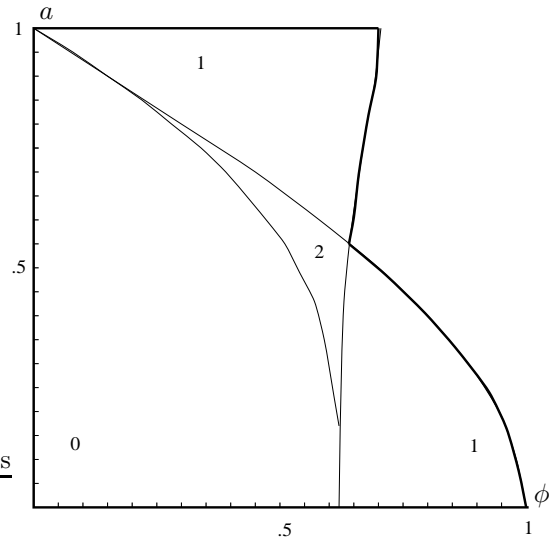


FIG. 24. Number of solutions of equation (39) with $\bar{\beta} = 1$, in the space $\phi \times a$, where a is given by equation (48) (see caption of figure 20).

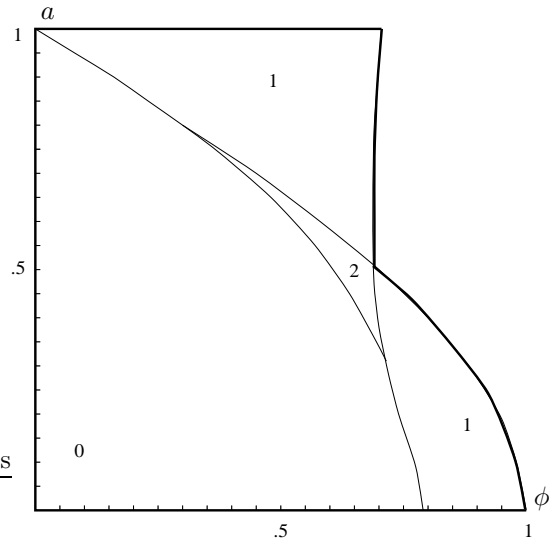


FIG. 25. Number of solutions of equation (39) with $\bar{\beta} = 2$, in the space $\phi \times a$, where a is given by equation (48) (see caption of figure 20).

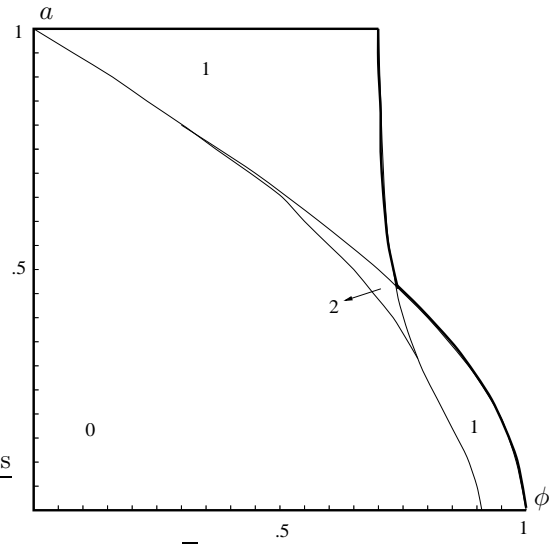


FIG. 26. Number of solutions of equation (39) with $\bar{\beta} = 5$, in the space $\phi \times a$, where a is given by equation (48) (see caption of figures 20).

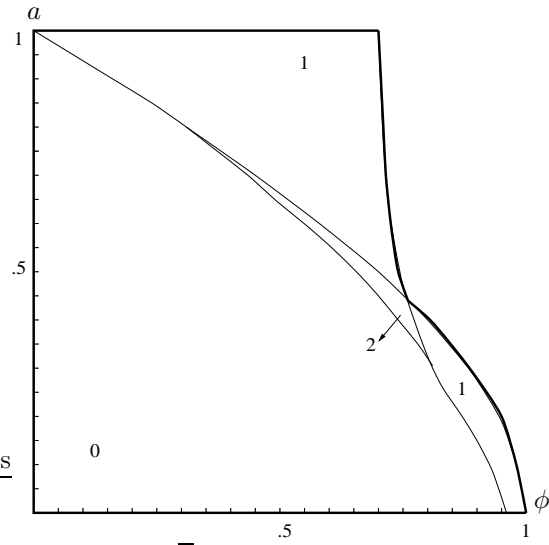


FIG. 27. Number of solutions of equation (39) with $\bar{\beta} = 10$, in the space $\phi \times a$, where a is given by equation (48) (see caption of figure 20).

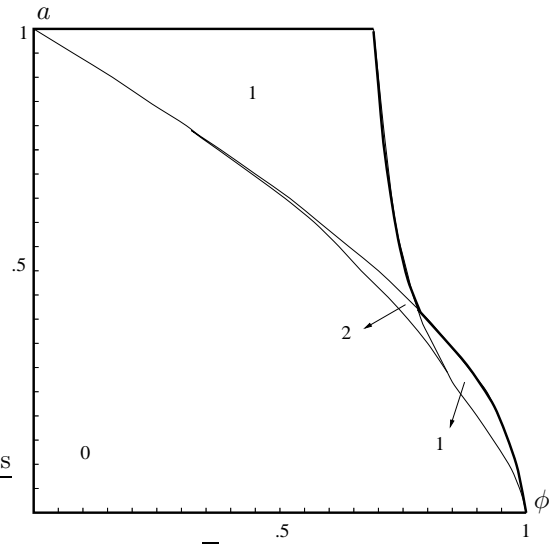


FIG. 28. Number of solutions of equation (39) with $\bar{\beta} = 100$, in the space $\phi \times a$, where a is given by equation (48) (see caption of figure 20).

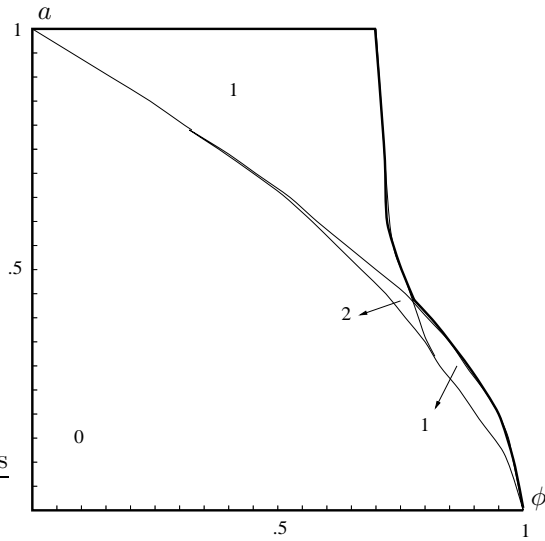


FIG. 29. Number of solutions of equation (39) with $\bar{\beta} = \infty$, in the space $\phi \times a$, where a is given by equation (48). Notice that for $\bar{\beta} = \infty$, equation (39) becomes (43) which corresponds to the extremal Reissner-Nordström-anti-de Sitter black hole, see discussion following equation (43) (see caption of figure 20).

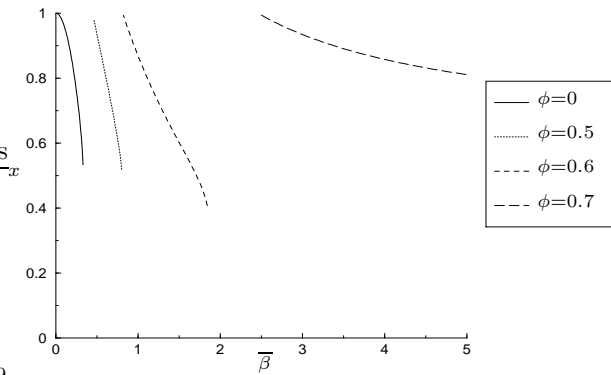


FIG. 30. Solutions of equation (39) which obey the stability condition (60), with $\bar{\alpha} = 1$, as a function of $\bar{\beta}$, for fixed values of the electrostatic potential at the boundary $\phi = 0, 0.5, 0.6, 0.7$. Comparing with figure 10, we can also recognize the unstable solutions.

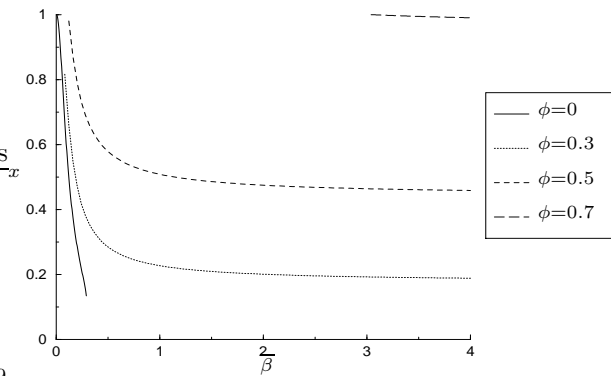


FIG. 31. Solutions of equation (39) which obey the stability condition (60), with $\bar{\alpha} = 5$, as a function of $\bar{\beta}$, for fixed values of the electrostatic potential at the boundary $\phi = 0, 0.3, 0.5, 0.7$. Comparing with figure 15, we can also recognize the unstable solutions.